HUNGARIAN AGRICULTURAL ENGINEERING
No 44/2025 17-28
Published online: http://hae-journals.org/
HU ISSN 0864-7410 (Print)
HU ISSN 2415-9751(Online)
DOI: 10.17676/HAE.2025.44.17
Received: 15.06.2025; Received in revised form: 15.08.2025;
Accepted: 25.08.2025; Available online: 10.09.2025.

PERIODICAL
OF THE COMMITTEE OF
AGRICULTURAL AND BIOSYSTEM ENGINEERING OF
THE HUNGARIAN ACADEMY OF SCIENCES
and
HUNGARIAN UNIVERSITY OF
AGRICULTURE AND
LIFE SCIENCES
INSTITUTE OF TECHNOLOGY

QUASI-STATIC BREAKAGE OF CORN PARTICLES

Author(s):
I. Keppler [1], J. Huang [1]

Affiliation:
[1] Institute of Technology - Hungarian University of Agriculture and Life Sciences (MATE), 2100 Gödöllő, Páter Károly u. 1., Hungary;

Email address:
keppler.istvan@uni-mate.hu; junhao.huang@phd.uni-mate.hu

Abstract: This study investigates the quasi-static fracture behavior of individual corn kernels under uniaxial compression. Experiments were conducted using an Instron 5965 universal testing machine at a loading rate of 1 mm min^{-1} on four geometrically different kernel types: elongated, flat, square, and round. The recorded force–displacement curves revealed a four-stage fracture process involving elastic deformation, micro-damage initiation, progressive crack propagation, and final crushing. The results show that kernel geometry has a significant effect on compressive strength and fracture energy, with elongated kernels exhibiting the highest mean load (≈ 580 N) and round kernels showing the most stable response. The absorbed fracture energy ranged between 0.17 and 0.22 mJ per kernel. These findings provide a quantitative foundation for calibrating discrete element method (DEM) simulations of kernel breakage under storage and handling conditions, contributing to more accurate prediction of mechanical damage in bulk grain systems.

Keywords: agricultural materials, corn kernel, quasi-static compression, fracture, mechanical damage

1. Introduction

The mechanical behavior of corn kernels is a key factor that influences both product quality and process efficiency throughout harvesting, handling, drying, and storage. During these stages, mechanical damage may lead to a reduction in germination rate, increasing susceptibility to fungal infection, and degradation of overall grain quality. While a large portion of mechanical damage originates from impact or high-rate loading events during harvesting and transportation, a substantial amount of kernel breakage also occurs under quasi-static conditions. For example, due to compaction and self-weight during long-term storage or mechanical pressure in silos [1], [2].

It is valuable to understand the quasi-static fracture behavior of corn kernels in order to predict storage losses and develop handling and drying systems that are safer and more energy efficient. The failure of impact-induced is dominated by inertial effects and localized stress concentrations, while quasi-static compression involves slow deformation where viscoelastic and structural anisotropies govern the mechanical response. The damage patterns are typically indeterminate: internal cracking, pericarp delamination, or gradual crushing of the endosperm may develop without complete kernel fragmentation [3].

Previous studies on corn kernel mechanics have mainly focused on dynamic or impact loading, seeking correlations between impact energy, moisture content, and the probability of visible damage. Far fewer investigations have examined the quasi-static compression behavior of kernels with different shapes and geometries, even though kernel shape strongly affects local stress distribution, contact area, and the onset of fracture.

The present study aims to characterize the quasi-static compression and breakage behavior of corn kernels belonging to four distinct shape categories. The tests were performed under controlled compression rates using an Instron universal testing machine, which records complete force–displacement curves until failure. The objective is to quantify how kernel geometry and loading rate influence the mechanical response and

fracture characteristics, and to provide a reliable experimental basis for the calibration of particle-scale models and the assessment of damage risks during grain storage.

2. Fracture process under quasi-static loading

In the mechanical compression of biological grains, two principal loading modes can be distinguished: dynamic impact and quasistatic compression loadings [4]. Under impact loading,

The rapid failure and fragmentation along the existing cracks and flaws due to the inertial effects, which dominate breakage, and then the crack propagation through the kernel. The process of grain breakage is strongly influenced by impact velocity and kernel moisture content, as reported by various studies on agricultural particle damage under impact and compression [5].

In contrast, during quasi-static compression, the deformation rate is sufficiently low that inertial effects become negligible. The kernel deforms gradually, allowing viscoelastic and structural heterogeneities to control the stress distribution and fracture initiation. In this regime, failure usually proceeds through local crushing, pericarp delamination, and internal cracking, rather than by complete disintegration. The progressive evolution of the contact area between the kernel and the loading plate significantly affects the stress field. The microstructure consists of the pericarp, aleurone layer, and starchy endosperm, which play a critical role in determining how cracks initiate and propagate within the grain body [6].

The quasi-static fracture process can be divided into several characteristic stages:

1. Elastic compression – At the beginning of deformation, the kernel behaves elastically, and the stress–strain response is nearly linear.
2. Micro damage initiation – At the load increasing phase, internal cracks begin to slip, which leads to stiffness reduction.
3. Crack propagation and delamination – Cracks develop through the endosperm, which causes a gradual loss of stiffness and energy dissipation.
4. Ultimate crushing – The kernel totally fractures since the external stress or strain exceeds the strength. The force–displacement curve typically exhibits a peak load followed by a sudden drop [7].

These stages correspond well to experimental results obtained from the corn grain breakage under controlled quasi-static loading conditions. Zhou [3] found that kernel shape and orientation strongly affect the maximum load and energy dissipation. The detailed review by Chen et al. [6] emphasizes that although dynamic fracture receives more attention in the context of harvesting and processing aspects, quasi-static failure mechanisms are equally important. Because quasi-static governs the long-term breakage and degradation of kernels during storage and compaction.

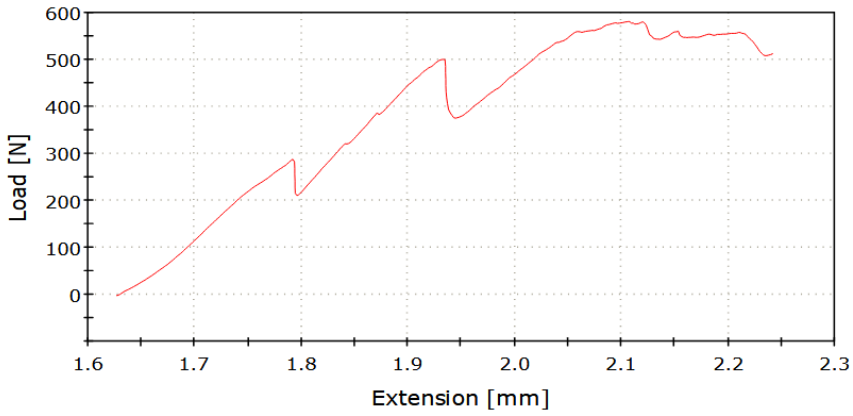

Figure 1. Typical quasi-static compression curve of a corn kernel

Figure 1. shows a representative load–extension curve obtained during the quasi-static compression of a single corn kernel. The force-displacement curve illustrates the four characteristic stages of the fracture process. First, a nearly linear rise in load corresponds to elastic compression, where deformation is reversible and governed by the contact stiffness. The first sudden drop in the curve indicates the rise of micro damage initiation, which is probably due to local cracking of the pericarp or minor delamination within the

endosperm. The reappearance of multiple partial loads is due to the continuous compression, which also represents crack propagation and delamination. At the same time, new contact surfaces form to redistribute the compressive stress. Finally, the force reaches the maximum value, followed by a soft plateau and partial relaxation, which corresponds to ultimate crushing, where the kernel loses structural integrity and collapses. The multi-peak pattern confirms that failure develops progressively through local damage events rather than by a single catastrophic fracture, which is typical for quasi-static loading of agricultural materials [3], [6], [7], [8], [9].

Figure 2. shows a typical failure morphology observed after quasi-static loading. The kernel exhibits partial crushing and delamination of the pericarp, with visible internal cracking in the endosperm. Such failure patterns confirm the progressive nature of quasi-static fracture, where multiple local damage events occur before complete structural collapse.

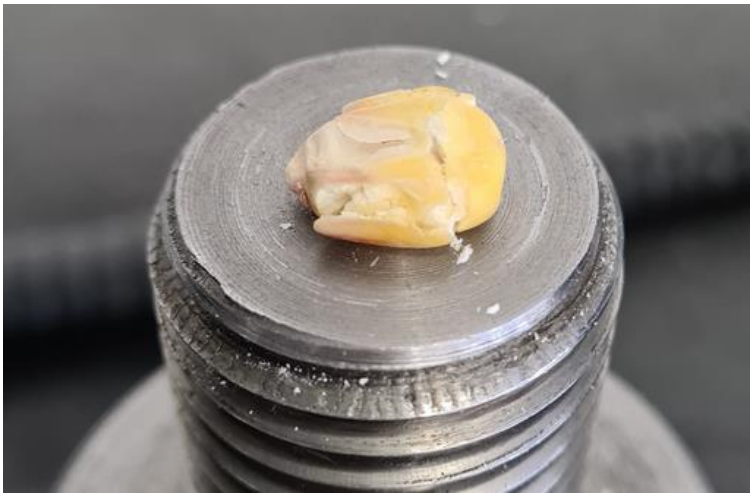

Figure 2. Corn kernel after quasi-static compression test

3. Mechanical interpretation of quasi-static fracture

The mechanical process of kernel fracture under quasi-static compression can be interpreted through classical energy and stress-based formulations. The overall response involves an initial elastic stage, a non-linear damage initiation phase, and the final crushing, in which energy dissipation and internal cracking dominate.

In the initial stage, the force–displacement relation can be approximated as linear elastic:

$$F = k\,\delta$$

where F is the applied load, δ is the platen displacement, and k is the effective stiffness of the kernel–platen contact system. The stored strain energy up to the onset of micro-damage (δ_c) is:

$$U = \frac{1}{2} k \delta_c^2.$$

When the local stress at internal flaws exceeds the cohesive strength, micro-cracks begin to develop, and part of this stored energy is released as fracture energy.

The condition for crack propagation follows Griffith's energy criterion [7]:

$$G = -\frac{\partial \Pi}{\partial A} \geq G_c$$

where G is the energy release rate, A is the crack surface area, and G_c is the critical fracture energy (or toughness). Once G exceeds G_c, cracks propagate and merge, leading to structural degradation of the kernel.

The total mechanical work performed during the compression test is the area under the load–load-displacement curve:

$$W = \int_0^{\delta_f} F(\delta)\mathrm{d}\delta.$$

where δ_f is the displacement at failure.

The fracture energy, or specific breakage energy per unit mass, is then:

$$E_b = \frac{W}{m},$$

where m is the mass of the tested kernel. Experimental studies have shown that E_b depends on the kernel shape, loading direction, and moisture content [3], [9]. Higher moisture generally increases ductility and energy absorption capacity, while irregular or elongated shapes tend to concentrate stress and fail at lower energy.

During loading, the local contact area A_c evolves, influencing the effective compressive stress:

$$\sigma_{eff} = \frac{F}{A_c(\delta)}.$$

Since A_c increases with deformation in quasi-static loading, stress concentration is partially mitigated, allowing multiple local damage events before catastrophic failure. This behavior explains the multi-peak load–extension pattern observed in Figure 1.

Biological materials such as corn kernels exhibit viscoelastic and rate-dependent responses. The Kelvin–Voigt model can describe the time-dependent strain $\varepsilon(t)$ under applied stress $\sigma(t)$ [8]:

$$\sigma(t) = E\varepsilon(t) + \eta\frac{\mathrm{d}\varepsilon(t)}{\mathrm{d}t},$$

where E is the elastic modulus and η is the viscosity coefficient.

At low strain rates (quasi-static compression), viscous effects contribute to energy dissipation, producing gradual crack propagation and a smooth post-peak decay instead of abrupt fracture typical of high-rate impacts.

The experimental and analytical description of kernel fracture provides essential parameters and physical insight for building a realistic DEM model. The fracture-mechanical interpretation—through quantities such as fracture energy E_b, peak stress, and energy release rate G_c defines the material's resistance to crack initiation and propagation. These quantities can be directly related to the microscale parameters used in DEM, such as bond normal and shear strength, inter-particle stiffness, and cohesive energy density[8], [10], [11].

In practice, DEM models represent each kernel as an assembly of bonded elements whose collective behavior reproduces the macroscopic fracture response. The calibration process ensures that the energy dissipated by bond breakage per unit mass equals the measured fracture energy:

$$E_b \approx \frac{1}{m}\sum_i U_{b,i}^{\mathrm{break}},$$

where $U_{b,i}^{\mathrm{break}}$ is the elastic energy stored in bond i at failure. This equivalence connects the continuum-scale fracture energy E_b from experiments to the discrete bond energy parameters in DEM. Furthermore, the experimentally observed typical load-displacement curve (Figure 1.) and the identified deformation stages (elastic, micro-damage, crack propagation, and ultimate crushing) serve as benchmarks for model validation. A properly calibrated DEM model should reproduce not only the peak force and stiffness but also the progressive multi-peak pattern that characterizes quasi-static fracture of corn kernels [11], [12]. Thus, the fracture-mechanics framework provides the theoretical foundation for interpreting DEM parameters in

physical terms, ensuring that the microscale model reflects the experimentally observed macroscopic behavior.

The Discrete Element Method (DEM) is a computational framework used to simulate granular materials by representing each grain as an individual entity whose motion and contact forces obey Newton's laws. Contact interactions are governed by force–displacement relationships that capture elastic, frictional, and damping effects. For modeling grain fracture, however, additional formulations are required to represent intra-particle stress, crack initiation, and fragmentation phenomena. Two general strategies exist: the Bonded Particle Model (BPM) and the Particle Replacement Method (PRM). In BPM, each particle is represented by a cluster of smaller bonded sub-particles; when a bond fails, the cluster disintegrates [13], [14]. In PRM, an intact particle is replaced by fragments once a stress- or energy-based failure criterion is reached [14], [15]. Both methods have been implemented in Rocky DEM and are widely used for modeling biological material breakage.

Rocky DEM provides polyhedral and multi-sphere particle representations, both of which can describe the irregular geometry of corn kernels. In this study, kernels are represented as bonded clusters to allow crack formation within the particle. The simulation workflow includes: (1) importing or constructing realistic kernel geometries, (2) assigning mechanical and contact parameters (stiffness, friction, damping, cohesion), (3) defining the breakage criterion based on tensile or shear bond strength, and (4) monitoring the evolution of contact networks and fragment formation.

Zhang et al. (2024) [12] developed a polyhedral DEM model of corn kernels in Rocky DEM and demonstrated accurate reproduction of contact stress and packing behavior. Similarly, Zeng et al. [5] presented a generalized approach for DEM breakage modeling using a bonding particle model, which has since been applied to granular and agricultural materials.

Accurate breakage modeling requires calibration against experimental data. Typical calibration parameters include contact stiffness, bond normal and shear strength, friction coefficients, damping ratios, and restitution coefficients. These parameters are tuned so that simulated peak load, energy absorption, and failure displacement match measured compression tests.

Xu et al. (2025) [11] proposed a meta-modelling approach for calibrating breakable corn kernel DEM models, achieving 0.6–10 % deviation in rupture force compared to experiments. Validation should include not only mechanical response (force–displacement curves) but also qualitative aspects such as crack pattern and fragment size distribution. Chen et al. (2024) [16] emphasized that model verification against multiple test types (single kernel, bulk compression) is essential for predictive reliability.

Several practical challenges exist in simulating the quasi-static fracture of biological particles:

- Shape realism. The complex geometry of kernels significantly affects contact stress. Simplified spherical models underestimate local stress concentrations, while polyhedral or bonded-cluster representations capture realistic fracture modes [17].
- Quasi-static conditions. DEM is inherently dynamic; to emulate quasi-static compression, very small time steps, adequate damping, and low platen velocities must be used to suppress inertial effects.
- Computational cost. Bonded clusters can consist of hundreds of sub-particles per kernel, leading to heavy computational loads. Hybrid or coarse-grained approaches may be applied to maintain feasibility.
- Failure criterion selection. Stress-, strain-, or energy-based criteria yield different breakage patterns. The choice must be guided by experiments and sensitivity analysis [18].
- Biological variability. Natural scatter in kernel geometry, density, and internal structure must be represented statistically to reproduce the experimental dispersion of rupture forces.

Once calibrated, the Rocky DEM model can simulate bulk assemblies of corn kernels under slow compression, storage pressure, or handling processes. Such simulations can reveal the spatial distribution of contact forces, predict the fraction of broken kernels, and support the design of safer storage and conveying systems. Related DEM investigations have also addressed impact-induced kernel breakage, demonstrating the influence of impact velocity on internal cracking and overall damage evolution [19].

4. Experimental investigations

Quasi-static compression tests were performed using an Instron 5965 universal testing machine, equipped with a 5 kN load cell suitable for agricultural and biological materials. The load cell has a measurement accuracy of ±5 N, which ensures accurate force recording even during low-force preloading stages. The tests

were conducted by controlling displacement, and the applied force and platen displacement were recorded continuously at a sampling rate of 100 Hz.

Corn kernels were classified into four shape groups based on visual morphology and aspect ratios: elongated, flat, round, and square (Figure 3.). Each group represented a distinct geometric type typically found within commercial hybrid maize. The classification followed visual sorting under consistent lighting, and representative samples were photographed and measured before testing.

elongated flat square round

Figure 3. Corn kernel morphological classification

For each shape category, the compression tests were carried out at the quasi-static loading rate of 1 mm min^{-1}, corresponding to quasi-static deformation conditions. The kernels were placed individually between two parallel, polished steel platens, with their longest axis aligned vertically (loading direction). Tests were continued until a clear load drop occurred on the force–displacement curve, indicating fracture or crushing of the kernel.

Each measurement provided a complete force–displacement curve, from which the maximum compression force, stiffness (initial slope), and energy absorption until fracture were derived. These quantities were later used for correlation with kernel shape and for calibration of the DEM model. The corn kernels were previously dried to storage moisture content to ensure long-term grain storage. All samples were stored at room temperature (22 ± 1 °C) and ambient relative humidity (40–45 %) for at least 24 hours before testing to minimize moisture gradients. The average moisture content of the kernels was approximately 12–13 % measured by a grain moisture meter before the tests.

5. Results

The results of the quasi-static compression experiments are presented and analyzed in this section. Each kernel was subjected to uniaxial loading under controlled conditions, and the corresponding force–displacement responses were recorded. The obtained data allows the identification of characteristic stages of deformation and fracture, as well as the evaluation of mechanical parameters such as maximum load, stiffness, and energy absorption.

The analysis focuses on representative samples selected from each morphological group, highlighting typical features of the load–extension curves and their variability. The discussion first examines the detailed behavior of a representative elongated kernel, followed by a statistical summary of the test series.

In Figure 4., the force–displacement response spans roughly 1.7–2.8 mm of extension and reaches a peak load ≈ 700 N. An initial steep, near-linear rise (≈2.1–2.35 mm) indicates elastic compression and growth of the contact area. A first modest load drop follows (micro-damage initiation), after which the curve re-hardens and continues to climb. Between about 2.1 and 2.6 mm the signal shows several pronounced secondary peaks and partial recoveries, consistent with crack propagation and local delamination within the kernel. The local maximum occurs near mid-span of this region (≈2.5 mm), followed by a staircase-like post-peak decay with small recoveries up to ≈2.65–2.75 mm, marking ultimate crushing and progressive loss of stiffness. This multi-peak, stepwise pattern is characteristic of quasi-static, progressive fracture in dried kernels: failure proceeds through successive local events rather than a single catastrophic break.

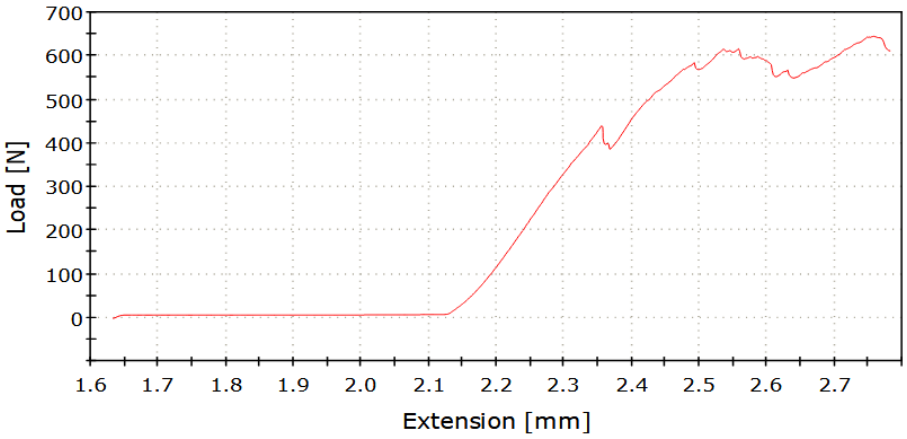

Figure 4. Typical force–displacement curve of an elongated kernel at 1 mm min^{-1} loading rate

A total of ten elongated kernels were tested under the quasi-static loading rate of 1 mm min^{-1}. The recorded force–displacement curves showed similar qualitative behavior, with an initial linear elastic phase followed by multiple partial load drops prior to final crushing. Despite the inherent biological variability, the force–displacement responses were reproducible in terms of their general shape and characteristic failure sequence.

The maximum compression force values ranged from approximately 200 N to 1000 N, with an average of 580 N and a standard deviation of 220 N. The coefficient of variation (COV) of about 38 % reflects the natural heterogeneity of kernel geometry and internal structure. Specimens with thinner or flatter morphology tended to fracture at lower loads, whereas thicker, more compact kernels sustained significantly higher forces before failure.

The mean deformation at peak load was around 2.4 mm, corresponding to an average strain of approximately 6–8 %, depending on kernel dimensions. The fracture energy—approximated by the area under the force–displacement curve—was estimated between 0.10 mJ and 0.35 mJ per kernel, with a mean value of 0.22 mJ.

Statistical analysis revealed that the scatter in the results mainly originates from microstructural differences such as pericarp thickness, internal voids, and endosperm hardness. These variations are typical for dried kernels and confirm that fracture occurs through multiple local cracking events rather than by a single, well-defined stress threshold.

Figure 5. displays the representative compression curve of a flat-type corn kernel. The loading response extends over approximately 1.3–2.8 mm of displacement and reaches a peak load of about 700 N. The initial segment (from 2.05 to ≈ 2.25 mm) shows a steep, nearly linear increase in load, corresponding to elastic compression of the kernel between the parallel platens. This is followed by a short plateau and a first force drop, which indicates micro-damage initiation, most likely the onset of pericarp cracking.

Between roughly 2.2 mm and 2.5 mm, multiple minor peaks appear as the internal structure fails progressively; this stage represents crack propagation and local delamination of the pericarp–endosperm interface. The staircase-like post-peak softening reveals a progressive, quasi-brittle failure rather than an abrupt break typical of dynamic loading.

The absorbed energy (area under the curve) was approximately 0.20 mJ. The pattern confirms that, even in flat kernels with larger contact area and smaller thickness, fracture proceeds through successive micro-failures and localized crushing rather than a single rupture event.

Ten flat kernels were analyzed at the same quasi-static loading rate. The maximum compression forces ranged between 250 N and 750 N, with an average of 460 N and a standard deviation of 160 N (COV ≈ 35 %). The average displacement at peak load was 2.1 mm, and the mean absorbed energy reached 0.17 mJ.

Compared with the elongated group, flat kernels showed lower peak loads and slightly smaller deformation capacity, which can be attributed to their larger initial contact area and thinner geometry. The mechanical response was less steep in the elastic region, implying lower stiffness, and the onset of cracking occurred earlier in the loading cycle.

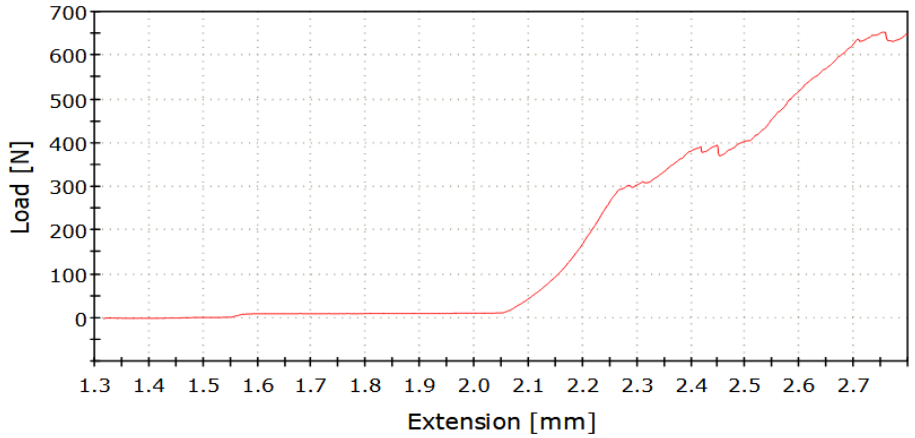

Figure 5. Typical force–displacement curve of a flat kernel at 1 mm min^{-1} loading rate

The moderate variability within the flat group reflects differences in pericarp thickness and internal micro-voids, both of which influence local stress distribution. Nevertheless, the general trend and average parameters are consistent with previously reported quasi-static compression tests on dried maize kernels.

Figure 6. shows the representative force–displacement curve of a square-type kernel compressed at 1 mm min^{-1}. The response extends from 1.7 mm to 2.4 mm displacement and reaches a peak load of about 600 N. The initial linear region up to ≈ 1.9 mm represents elastic compression and contact-area growth. A first load drop near 1.95 mm indicates micro-damage initiation, followed by two distinct re-hardening phases and secondary maxima around 2.1 and 2.3 mm. These oscillations reflect crack propagation and localized crushing within the kernel's endosperm. After the global maximum, the force decreases gradually with minor fluctuations, signaling progressive crushing and residual load transfer between intact zones. The deformation before final collapse was roughly 0.7 mm, and the absorbed energy (area under the curve) was about 0.18 mJ. The shape of the curve—steep initial rise, two or three successive peaks, and a soft post-peak region—confirms a quasi-brittle, stepwise fracture process, consistent with the dried, dense structure of the square kernels.

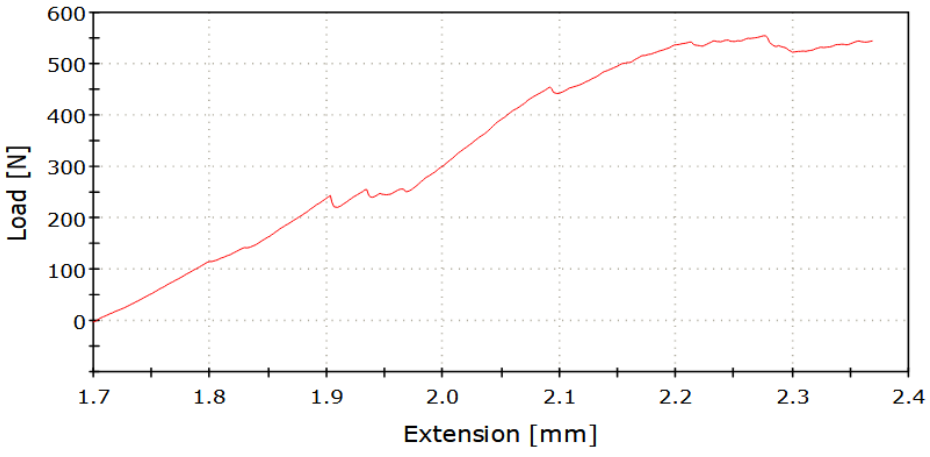

Figure 6. Typical force–displacement curve of a square kernel at 1 mm min^{-1} loading rate

Ten square kernels were tested under the same quasi-static loading rate. The maximum loads ranged from 280 N to 1000 N, with a mean value of 520 N and a standard deviation of 210 N (COV ≈ 40 %). The average displacement at peak load was 2.3 mm, and the mean absorbed energy was 0.19 mJ. Compared with the elongated and flat groups, the square kernels exhibited intermediate strength and relatively balanced stiffness, which can be attributed to their more symmetrical geometry and uniform stress distribution under

compression. The multipeak responses were slightly less pronounced than in elongated kernels, implying that square kernels fracture through fewer, larger damage events rather than many small micro-cracks.

This behavior supports the idea that geometric compactness reduces internal stress concentration, delaying complete failure.

Figure 7. presents the characteristic compression curve for a round-type corn kernel.

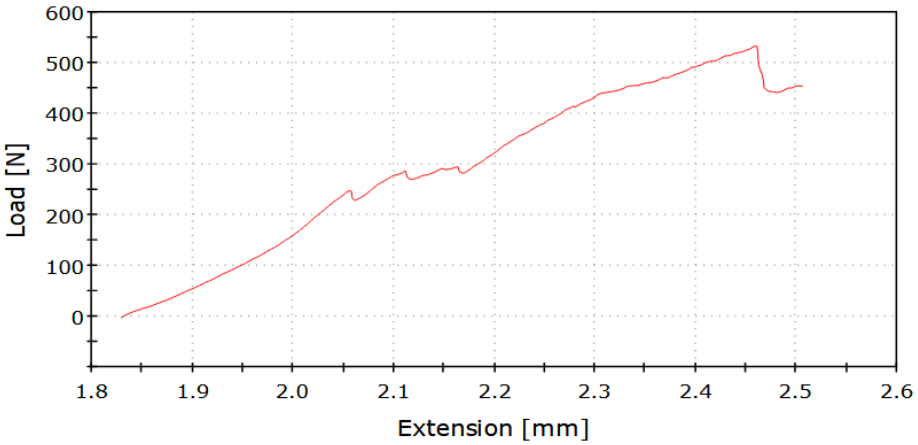

Figure 7. Typical force–displacement curve of a round kernel at 1 mm min^{-1} loading rate

The total displacement spans 1.8–2.6 mm, and the peak load reaches about 600 N. A nearly linear increase in force is observed up to ≈ 2.0 mm, representing elastic compression and uniform stress build-up due to the symmetrical geometry. A small drop near 2.05 mm marks the initiation of micro-damage, likely at the contact zones where the curved surface first flattens. Between 2.1 mm and 2.4 mm the curve exhibits two secondary maxima separated by partial relaxations—signatures of crack propagation and localized crushing of the endosperm. After the global maximum, the load decreases gradually, showing a soft post-peak tail typical of progressive crushing rather than abrupt brittle failure. Because of their nearly spherical shape, round kernels distribute stresses more evenly; the onset of fracture occurs at higher deformations relative to their size, but the final collapse is more stable and less jagged than for elongated or flat kernels. The deformation before final failure was ≈ 0.8 mm, and the estimated fracture energy (area under the curve) was about 0.21 mJ.

Ten round kernels were tested under quasi-static loading. The maximum loads varied between 150 N and 650 N, yielding a mean F_{max} ≈ 370 N with a standard deviation ≈ 150 N (COV ≈ 41 %). The mean displacement at peak load was 2.3 mm, and the average absorbed energy reached 0.19 mJ. Compared with the other shape categories, round kernels exhibited lower stiffness and moderate strength, but the most stable and reproducible fracture curves, due to their isotropic geometry and uniform stress field. The smaller scatter in the mid-range loads suggests that geometric uniformity dominates over local material heterogeneity.

Nevertheless, slight asymmetries or flattened zones still cause multiple minor cracking events, confirming that failure develops through distributed micro-damage rather than a single global break. This agrees with the observation that kernel strength is closely related to pericarp thickness and seed-coat morphology [20].

The quasi-static compression tests revealed that all kernel types-elongated, flat, square, and round-exhibited a similar four-phase fracture behavior: an initial elastic stage, the onset of micro-damage, progressive crack propagation, and final crushing. However, the quantitative responses differed considerably depending on geometry. Elongated kernels generally showed the highest peak forces and most pronounced multipeak patterns, reflecting anisotropic stress distribution and multiple internal failure zones. Flat kernels failed at lower loads and smaller deformations due to their larger contact area and reduced thickness, while square kernels displayed intermediate strength and balanced stiffness, consistent with their more symmetrical shape. Round kernels, although mechanically weaker on average, exhibited the most stable and reproducible force–displacement curves, with smoother post-peak decay and fewer sharp drops.

Overall, the results confirm that kernel geometry strongly influences the mechanical response under quasi-static loading, both in terms of load capacity and energy dissipation. The progressive, multi-event fracture observed across all groups emphasizes the need for DEM models that incorporate distributed bond failure and variable cohesive strength, rather than a single uniform breakage criterion. These findings provide a

consistent experimental foundation for calibrating and validating particle-scale simulations of corn kernel breakage under storage-related mechanical stresses. These findings are consistent with the cyclic breakage behavior reported for corn kernels subjected to repeated loadings under quasi-static compression [21].

6. Conclusions

The quasi-static compression experiments performed on corn kernels of different shapes demonstrated that the fracture behavior of dried kernels is strongly geometry-dependent yet governed by the same fundamental sequence of elastic deformation, micro-damage initiation, crack propagation, and ultimate crushing (Table 1.).

Table 1. Summary of quasi-static compression results

Kernel type	Mean F_{max} [N]	Std. dev [N]	Mean deformation [mm]	Mean Energy [mJ]	Typical feature
Elongated	580	220	2.4	0.22	Strong multipeak, progressive cracking
Flat	460	160	2.1	0.17	Early cracking, low stiffness
Square	520	210	2.3	0.19	Balanced stiffness, few large cracks
Round	370	150	2.3	0.19	Smooth curve, isotropic crushing

Summarizing the conclusions:

- Elongated kernels exhibited the highest compressive strength, with average peak forces around 580 N and pronounced multi-peak load-displacement responses indicating successive internal failures.
- Flat kernels showed lower mean strength (≈ 460 N) and smaller deformation capacity, failing earlier due to broader contact area and reduced wall thickness.
- Square kernels displayed intermediate mechanical resistance (≈ 520 N) and balanced stiffness, their symmetry leading to more uniform stress distribution and fewer micro-crack events.
- Round kernels had the lowest mean peak force (≈ 370 N) but yielded the most consistent, smooth fracture curves, suggesting isotropic stress distribution and stable crushing behavior.
- The absorbed fracture energy ranged between 0.17 and 0.22 mJ per kernel, with the elongated and round types showing the highest energy dissipation. The observed multi-stage, quasi-brittle fracture confirms that mechanical failure in dried corn kernels proceeds progressively through distributed cracking, rather than a single catastrophic rupture.

These experimental findings provide a robust reference for calibrating Discrete Element Method (DEM) models of kernel breakage in Rocky DEM. The results highlight the need to incorporate variable bond strength and distributed cohesion within the DEM framework to reproduce the experimentally observed scatter and multi-peak behavior. This integration will allow more realistic simulation of grain handling, compaction, and storage-induced breakage processes.

Future research should aim to extend the present findings in three main directions:

1. Moisture dependence. The present tests were performed on kernels dried to storage moisture. Investigating the same loading regime at higher and lower moisture levels will quantify the role of viscoelastic softening and crack bridging on quasi-static fracture energy.
2. Dynamic comparison. Complementary high-rate compression or impact tests would enable direct comparison between quasi-static and dynamic failure regimes, providing a complete fracture envelope for DEM model validation.
3. Numerical upscaling. Incorporating the calibrated breakage model into bulk-scale DEM simulations of grain compaction and silo storage will allow prediction of cumulative breakage ratios under realistic load conditions. Coupling DEM with finite element (FEM) or continuum models could further enhance predictive capability.

In addition, X-ray micro-CT or digital image correlation (DIC) techniques could be applied to visualize internal cracking during compression and to refine the spatial distribution of cohesive parameters in the DEM framework. Future studies could also incorporate fractal-based metrics to describe the irregularity and scaling behavior of kernel fracture surfaces [22].

Such developments will bridge the gap between laboratory-scale experiments and full-scale simulation of grain-handling systems, contributing to the optimization of post-harvest processes and the reduction of mechanical damage in storage and transport.

Acknowledgement

The study was supported by 2019-1.1.1-PIACI-KFI-2019-00101. This study was also supported by the China Scholarship Council (CSC) and the Stipendium Hungaricum Scholarship program.

References

[1] **S. Garneoui, I. Keppler, P. Korzenszky, and M. S. Talafha** (2021) "Numerical study on the impact of particles filling pattern and screw parameters on the mixing uniformity of wheat grains in a screw mixer," *Appl. Comput. Mech.*, vol. 15, no. 2, doi: 10.24132/acm.2021.689.

[2] **R. Bartosik, H. Urcola, L. Cardoso, G. Maciel, and P. Busato** (2023) "Silo-bag system for storage of grains, seeds and by-products: A review and research agenda," *J. Stored Prod. Res.*, vol. 100, p. 102061, Jan. 2023, doi: 10.1016/j.jspr.2022.102061.

[3] **Z. Mengmeng and S. Huinan** (2024) "Experimental study on corn grain crushing via quasi-static compression method," *Trans. Chin. Soc. Agric. Eng.*, vol. 40, no. 9, pp. 289–296.

[4] **Y. Han *et al.*,** "Breakage behaviour of single rice particles under compression and impact," *Adv. Powder Technol.*, vol. 32, no. 12, pp. 4635–4650, Dec. 2021, doi: 10.1016/j.apt.2021.10.017.

[5] **Y. Zeng, F. Jia, Y. Xiao, Y. Han, and X. Meng** (2019) "Discrete element method modelling of impact breakage of ellipsoidal agglomerate," *Powder Technol.*, vol. 346, pp. 57–69, Mar. 2019, doi: 10.1016/j.powtec.2019.01.082.

[6] **Z. Chen, C. Wassgren, and K. Ambrose** (2020) "A Review of Grain Kernel Damage: Mechanisms, Modeling, and Testing Procedures," *Trans. ASABE*, vol. 63, no. 2, pp. 455–475, doi: 10.13031/trans.13643.

[7] **A. A. Griffith** (1920) "The phenomena of rupture and flow in solids." pp. 163-198.

[8] **J. D. Ferry** (1980) "Viscoelastic Properties of Polymers." Wiley and Sons, New York, 1980.

[9] **W. Kruszelnicka** (2021) "Study of Selected Physical-Mechanical Properties of Corn Grains Important from the Point of View of Mechanical Processing Systems Designing," *Materials*, vol. 14, no. 6, p. 1467, Mar. 2021, doi: 10.3390/ma14061467.

[10] **K. Xu, W. Zhou, G. Ma, X. Chang, and L. Yang** (2018) "Review of particle breakage simulation based on DEM," *Chin. J. Geotech. Eng.*, vol. 40, no. 5, pp. 880–889.

[11] **J. Xu, Y. Yao, Y. Zhu, C. Sun, Z. Cao, and D. Geng** (2025) "Discrete Meta-Modeling Method of Breakable Corn Kernels with Multi-Particle Sub-Area Combinations," *Agriculture*, vol. 15, no. 15, p. 1620, July 2025, doi: 10.3390/agriculture15151620.

[12] **J. Zhang, X. Jiang, and Y. Yu** (2024) "Modeling Method of Corn Kernel Based on Discrete Element Method and Its Experimental Study," *Agriculture*, vol. 14, no. 12, p. 2195, Dec. 2024, doi: 10.3390/agriculture14122195.

[13] **Y. Su *et al.*,** (2022) "A combined experimental and DEM approach to optimize the centrifugal maize breakage tester," *Powder Technol.*, vol. 397, p. 117008, Jan. 2022, doi: 10.1016/j.powtec.2021.11.052.

[14] **N. Jiménez-Herrera, G. K. P. Barrios, and L. M. Tavares** (2018) "Comparison of breakage models in DEM in simulating impact on particle beds," *Adv. Powder Technol.*, vol. 29, no. 3, pp. 692–706, Mar. 2018, doi: 10.1016/j.apt.2017.12.006.

[15] **A. G. Chiaravalle, J. Piña, and I. M. Cotabarren** (2025) "DEM simulation of maize milling in a hammer mill," *Powder Technol.*, vol. 457, p. 120892, May 2025, doi: 10.1016/j.powtec.2025.120892.

[16] **Z. Chen, C. Wassgren, and R. P. K. Ambrose** "Development and validation of a DEM model for predicting compression damage of maize kernels," *Biosyst. Eng.*, vol. 230, pp. 480–496, June 2023, doi: 10.1016/j.biosystemseng.2023.05.004.

[17] **A. Patwa, R. P. K. Ambrose, and Mark. E. Casada** (2016) "Discrete element method as an approach to model the wheat milling process," *Powder Technol.*, vol. 302, pp. 350–356, Nov. 2016, doi: 10.1016/j.powtec.2016.08.052.

[18] **M. Prasanna and A. Polojärvi** (2023) "Breakage in quasi-static discrete element simulations of ice rubble," *Int. J. Mech. Sci.*, vol. 259, p. 108595, Dec. 2023, doi: 10.1016/j.ijmecsci.2023.108595.

[19] **Y. Yu *et al.*** (2025) "Modeling and simulation of impact and breakage of maize kernels based on the DEM-PBM," *Powder Technol.*, vol. 466, p. 121456, Dec. 2025, doi: 10.1016/j.powtec.2025.121456.

[20] **Ł. Gierz *et al.*** (2025) "Effects of Thickness of the Corn Seed Coat on the Strength of Processed Biological Materials," *Materials*, vol. 18, no. 2, p. 222, Jan. 2025, doi: 10.3390/ma18020222.

[21] **W. Kruszelnicka, P. Leda, A. Tomporowski, and K. Ambrose** (2024) "Breakage behavior of corn kernels subjected to repeated loadings," *Powder Technol.*, vol. 435, p. 119372, Feb. 2024, doi: 10.1016/j.powtec.2024.119372.

[22] **L. Xingping, W. Junyi, L. Yanan, X. Shendi, H. Jiarui** (2025) School of Agricultural Equipment Engineering, Henan University of Science and Technology, Luoyang 471003, Henan, China, "Fracture regularity of corn kernel and stalk based on fractal theory," *Int. J. Agric. Biol. Eng.*, vol. 18, no. 3, pp. 37–43, doi: 10.25165/j.ijabe.20251803.9222.